Logarithmic Dynamics and Aggregation in Epidemics

Franco Blanchini [a], Paolo Bolzern [b], Patrizio Colaneri [b,c], Giuseppe De Nicolao [d], Giulia Giordano [e]

***Abstract*—We consider a class of epidemiological models with an arbitrary number of infected compartments. We show that the logarithmic derivatives of the infected states converge to a consensus; this property rigorously explains the feature empirically observed in real epidemic data: the logarithms of the state variables associated with infected categories tend to behave as "parallel lines". We introduce and characterise the class of contagion functions, i.e., linear co-positive functions of the state variables that decrease (resp. increase) when the reproduction number is smaller (resp. larger) than 1. Finally, we analyse the generalised epidemiological model by considering the susceptible state variable along with a variable that aggregates all the infected compartments: this leads to an auxiliary planar system, governed by two differential inclusions, which has the same structure as the two-dimensional SI model and whose coefficients are functions of the original variables. We prove that well known properties of the classical SI model still hold in this generalised case.**

I. Introduction

We consider a general class of epidemiological models including an arbitrary number of infected compartments that are fed back by the dynamics of the susceptible population: each model can be described by a linear positive system along with a destabilising feedback loop through the flow of susceptible individuals, leading eventually to a positive bilinear system. The considered class of systems includes mean-field compartmental models of the SIR (Susceptible-Infected-Recovered) type, describing the spread of an infectious disease in a large, well-mixed population, see e.g. [2], [3], [9], [11], [15], [18], [19], [22], [24]. SIR-like systems were recently used to model the COVID-19 pandemic [12], [13], [17], [23], [27] and allow for the design of optimal control strategies to mitigate the spread of the infection [1], [4], [8], [5], [6], [16], [22], [20], [21], [25], [26], [28].

The particular structure of the considered class of models allows us to leverage the theory of positive linear systems, see e.g. [7], to identify relevant properties of these nonlinear (bilinear) systems. In particular:

- We show that the reproduction number $\mathcal{R}_0$, fundamental for the stability condition $S\mathcal{R}_0 < 1$, where S is the susceptible population, corresponds to the $\mathcal{H}_\infty$ norm of the open-loop linear positive system.
- We prove that relevant cost functions for the nonlinear system can be computed just based on the linear subsystem.
- We analyse the logarithmic dynamics of the system. Empirical data (we report e.g. the Italian COVID-19 pandemic data in 2020) show that the infected state variables, represented in a logarithmic scale, evolve as "parallel curves". We rigorously explain this observation by proving that the logarithm derivative vector obeys an ordinary-differential-equation system that asymptotically reaches a consensus.
- We define a contagion function as a linear co-positive function of all state variables that decreases (respectively, increases) when the reproduction number is smaller (respectively, larger) than 1. We provide a necessary and sufficient condition for a linear co-positive function to be a contagion function.
- By introducing an aggregate variable of all infected compartments, we derive an auxiliary planar system having the same structure as the standard two dimensional SI (Susceptible-Infected) model. The two coefficients of this system are not constant, as in the SI model, but are functions of the original state variables. We prove that well known properties of the classical SI model still hold in our generalised setting.

Notation: Throughout the paper we set $\mathbf{1}^\top = [1\ 1 \dots 1]$. For two vectors v and u, $u \ll v$ and $u \gg v$ ($u \leq v$ and $u \geq v$) respectively correspond to $u_k < v_k$ and $u_k > v_k$ ($u_k \leq v_k$ and $u_k \geq v_k$ for all k). The kth vector of the canonical basis is denoted as $\mathbf{e_k}$. For a vector v, $D(v) = \mathrm{diag}(v)$ denotes the diagonal matrix with v_i on the diagonal.

II. General properties of the model

We consider the class of models represented by equations:

$$\dot{x}(t) = Fx(t) + bu(t) \quad (1)$$
$$y(t) = c^\top x(t) \quad (2)$$
$$u(t) = S(t)y(t) \quad (3)$$
$$\dot{S}(t) = -S(t)y(t) \quad (4)$$
$$x(0) = x_0 \quad (5)$$
$$S(0) = S_0 \quad (6)$$

where $x(t) \in \mathbb{R}^n$, $u(t) \in \mathbb{R}$, $y(t) \in \mathbb{R}$. The variable S is the susceptible population fraction and x_i, $i = 1, 2, \dots, n$, are the population fractions in different infected compartments.

[a] University of Udine, Italy. blanchini@uniud.it
[b] Politecnico di Milano, Italy. paolo.bolzern@polimi.it, patrizio.colaneri@polimi.it
[c] IEIIT Consiglio Nazionale delle Ricerche
[d] University of Pavia, Italy. giuseppe.denicolao@unipv.it
[e] University of Trento, Italy. giulia.giordano@unitn.it

Remark 1. *Matrix F is characterised by parameters that represent the transition rates among the various infected compartments x. Vector c includes the contagion parameters, which depend on the non-pharmaceutical interventions (NPIs) adopted to contrast the spread of the infection.*

The parameters in F and c are assumed constant. We consider the following standing assumptions.

Assumption 1. *In system* (1)-(4)*,*

- *both vectors b and c are nonnegative;*
- *matrix F is Metzler and Hurwitz.*

System (1)-(4) is written in feedback form: it includes the open-loop linear positive system (1)-(2) and a nonlinear dynamic feedback given by (3)-(4), with $u = -\dot{S} \geq 0$. Closing the loop yields the equation

$$\dot{x}(t) = [F + bS(t)c^\top]x(t). \tag{7}$$

The susceptible variable $S > 0$ has a destabilising effect. The Frobenius-Perron eigenvalue $\mu(\bar{S})$ of $F + b\bar{S}c^\top$ is a monotonically increasing function of $\bar{S}$. Being F Hurwitz and Metzler, the smallest value $\bar{S}^*$ of $\bar{S}$ for which the Metzler matrix $F + b\bar{S}c^\top$ is no longer Hurwitz is characterised by the equation $\det(F + b\bar{S}c^\top) = 0$. Its solution,

$$\bar{S}^* = -\frac{1}{c^\top F^{-1} b},$$

is the inverse of the DC-gain of the transfer function $G(s) := c^\top(sI - F)^{-1}b$ of the system with input u and output y. For positive systems, $G(0)$ is the $\mathcal{H}_\infty$ (as well as the induced $\mathcal{L}_1$ and $\mathcal{L}_\infty$) input-output norm of such system. Therefore we are well advised to define the parametric reproduction number $\mathcal{R}_0$ as the $\mathcal{H}_\infty$ norm of the positive system from u to y with constant parameters, namely

$$\mathcal{R}_0 = -c^\top F^{-1} b. \tag{8}$$

Being the open-loop system positive, the $\mathcal{H}_\infty$ norm coincides with the induced $\mathcal{L}_1$ and $\mathcal{L}_\infty$ norms. For distributed epidemiological models including a contact network, $\mathcal{R}_0$ is a matrix, see e.g. [27]. Expression (8), proposed for the SIDARTHE model [12], is a generalisation of several well known expressions of the reproduction number; see e.g. [9, Section 9.5]. This number has the well known property that the stability of any equilibrium of system (7) with susceptible population $\bar{S}$ is equivalent to the condition

$$\mathcal{R}_0 \bar{S} < 1.$$

Among the fundamental properties of the reproduction number, we mention the following [2], [3], [5].

Proposition 1. *For any initial state (x_0, S_0), it holds that*

$$\lim_{t\to\infty} x(t) = 0 \quad \textit{and} \quad \lim_{t\to\infty} S(t) = \bar{S},$$

where $\bar{S}$ solves

$$\log\frac{S_0}{\bar{S}} - \mathcal{R}_0(S_0 - \bar{S}) = -c^\top F^{-1} x_0 > 0. \tag{9}$$

Consider now the cost

$$J(x_0, S_0) = \int_0^\infty l^\top x(t)dt - \gamma \int_0^\infty S(t)c^\top x(t)dt, \tag{10}$$

where $l \geq 0$, $\gamma > 0$. The positive term $l^\top x$ represents casualties or intensive-care-unit occupancy, while the negative integral coincides with $S_0 - \bar{S}$.

Proposition 2. *The cost* (10) *can be written as*

$$J(x_0, S_0) = q^\top x_0 + (q^\top b - \gamma)(S_0 - \bar{S}), \tag{11}$$

where $q = -l^\top F^{-1} \geq 0$.

Proof: Take $V(x, S) = q^\top x + q^\top bS$, so $\dot{V}(x, S) = q^\top(Fx - b\dot{S}) + q^\top b\dot{S} = -l^\top x$. The result follows after integrating both sides from 0 to ∞ and recalling that $\dot{S} = -Sc^\top x$ and, from Proposition 1, $x \to 0$ and $S \to \bar{S}$. ■

We can observe the following.

- Equation (9) enables to predict the final value $\bar{S}$ of $S(t)$ given the initial states x_0 and S_0. Function $g(\hat{S}, \mathcal{R}_0) = \log\frac{S_0}{\hat{S}} - \mathcal{R}_0(S_0 - \hat{S})$ is positive and decreasing in the interval $\hat{S} \in (0, 1/\mathcal{R}_0)$ and is zero for $\hat{S} = S_0$. Since $\omega_0 := -c^\top F^{-1} x_0 > 0$, there is a unique intersection, easy to compute, for $\bar{S} < 1/\mathcal{R}_0$. A graphical interpretation is in Figure 1.
- The value of $\bar{S} < \frac{1}{\mathcal{R}_0}$ satisfying $g(\bar{S}, \mathcal{R}_0) = \omega_0$ can be found as
$$\bar{S} = \frac{\log(\delta)}{\mathcal{R}_0}, \tag{12}$$
where $\kappa = \mathcal{R}_0 S_0 e^{-\mathcal{R}_0 S_0 - \omega_0}$ and $\delta \in (1, e^{1+\omega_0})$ is the unique solution of $\kappa\delta = \log(\delta)$.
- From equation (12) one can parametrise the set $\mathcal{S}$ of values $\bar{S}$ obtainable with a certain choice of $\mathcal{R}_0 \in \{\mathcal{R}_0^-, \mathcal{R}_0^+\}$ (recall Proposition 1). If $\hat{S} \in \mathcal{S}$ is a desired long-term *target fraction* of susceptible population, one can impose such a value by introducing NPIs that yield
$$\mathcal{R}_0 = \frac{\log(S_0/\hat{S}) + \omega_0}{S_0 - \hat{S}}.$$
- Proposition 2 is related to the induced $\mathcal{L}_1$ norm of the system with input u and output y. Assuming $x_0 = 0$, standard analysis of positive systems, see [7], yields
$$\sup_{u\in\mathcal{L}_1, u\neq 0} \frac{\int_0^\infty l^\top x(t)dt}{\int_0^\infty u(t)dt} = q^\top b.$$
Therefore, we have that
$$\frac{\int_0^\infty l^\top x(t)dt}{\int_0^\infty S(t)c^\top x(t)dt} = q^\top b + \frac{q^\top x_0}{S_0 - \bar{S}},$$
with $S_0 - \bar{S} \geq 0$ increasing with $\mathcal{R}_0$.

III. Logarithmic dynamics

Systems of the form (1)-(4) exhibit a peculiar behaviour: all the variables x_i, after an initial transient, tend to be

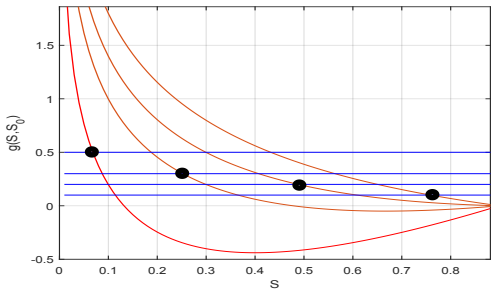

Figure 1: Function $g(\hat{S}, 0.9)$ associated with $\mathcal{R}_0 = -c(\bar{v})^\top F(\bar{p})^{-1} b = \{0.5, 1, 1.5, 2.5\}$ from top to bottom (red lines) and corresponding values (blue lines) of $\omega_0 = -c(\bar{v})^\top F(\bar{p})^{-1} x_0 = \{0.1, 0.2, 0.3, 0.5\}$. The black dots mark the values of $\bar{S}$ obtained by solving (9), or equivalently (12).

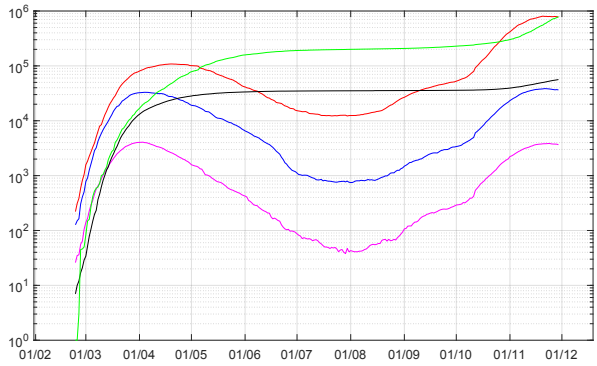

Figure 2: Real data curves (in logarithmic scale) showing the evolution of the COVID-19 pandemic in Italy from February to December 2020. The curves of pauci-symptomatic infected (red), hospitalised infected (blue), infected in intensive care units (purple) are essentially parallel. The integral variables of recovered (green) and deceased (black) are also shown.

proportional to each other, hence the plot of their logarithms tend to be "parallel curves". Precisely, we prove that

$$\lim_{t\to\infty} \frac{\dot{x}_k(t)}{x_k(t)} = \bar{\lambda}, \qquad \text{for all} \quad k,$$

namely to a common value. Then we argue that this behaviour is true after a transient for slowly varying pandemics.

The epidemic dynamics is captured by the time behaviour of the log-derivative functions of the infected variables:

$$\lambda = D(x)^{-1}\dot{x}. \tag{13}$$

where $D(v) = \mathrm{diag}(v)$. Given $\lambda(t)$, the vector of infected variables $x(t)$ satisfies

$$x(t) = e^{\int_0^t \lambda(\tau)d\tau} x_0. \tag{14}$$

Theorem 1. *The log-derivative vector λ in (13) satisfies the differential equation*

$$\dot{\lambda} = -\mathcal{L}(x, S)\lambda + D(x)^{-1} b \dot{S} c^\top D(x)\mathbf{1}, \tag{15}$$

where

$$\mathcal{L}(x, S) = D(x)^{-1}\left[D\left((F + bSc^\top)x\right) - (F + bSc^\top)D(x)\right]$$

is a Laplacian matrix: it has nonpositive off-diagonal entries and $\mathcal{L}(x, S)\mathbf{1} = 0$. The log-derivative vector λ reaches a consensus, i.e,

$$\lim_{t\to\infty} \lambda(t) = \bar{\lambda}\mathbf{1},$$

where $\bar{\lambda} < 0$ is the dominant (Perron-Frobenius) eigenvalue of the (Metzler and Hurwitz) matrix $F + b\bar{S}c^\top$. Moreover,

$$\lim_{t\to\infty} \frac{x_i(t)}{x_j(t)} = \frac{\bar{z}_i}{\bar{z}_j},$$

where $\bar{z}$ is the right (Perron-Frobenius) eigenvector of the (Metzler and Hurwitz) matrix $F + b\bar{S}c^\top$.

Proof: Consider the linear system $\dot{x} = (F + b\bar{S}c^\top)x$ where $\bar{S}$ is the equilibrium value of S computed via equation (9). Matrix $F + b\bar{S}c^\top$ is Metzler, Hurwitz and irreducible. Hence, it admits a Perron-Frobenius eigenvalue $\bar{\lambda} < 0$ associated with a strictly positive eigenvector, say $\bar{z}$, i.e. $(F + b\bar{S}c^\top)\bar{z} = \bar{\lambda}\bar{z}$. Taking $z(t) = \exp(\bar{\lambda}(t))x(t)$, it follows that $z(t) \gg 0$ for any $x_0 \gg 0$ and $z(t) \to \bar{z}$ for $t \to \infty$. Hence, all ratios x_i/x_j are bounded and converge to $\bar{z}_i/\bar{z}_j$. Now, consider equation (15) with $S = \bar{S}$, $x = 0$ and $x_i/x_j = \bar{z}_i/\bar{z}_j$. We have $\dot{\lambda} = -\mathcal{L}(\bar{z}, \bar{S})\lambda$ with $\mathcal{L}(\bar{z}, \bar{S}) = D(\bar{z})^{-1}\left[D\left((F + b\bar{S}c^\top)\bar{z}\right) - (F + bSc^\top)D(\bar{z})\right]$, so that $\lim_{t\to\infty} \lambda(t) = \bar{\lambda}\mathbf{1}$. ■

In the proof of Theorem 1, we essentially exploit the fact that, for $\dot{S} = 0$, $\lim_{t\to\infty} \lambda(t) = \bar{\lambda}\mathbf{1}$. The result is asymptotic; however, under controlled pandemic events, $S(t)$ varies slowly with respect to $x(t)$.

In realistic situations, $\dot{S}$ is expected to be very small. Considering e.g. the Italian population, a 0.2% daily variation of S means more than 10^5 new infected individuals per day: during the COVID-19 pandemic in 2020, in the absence of a vaccine, this would have led to more than 1000 new intensive-care-unit hospitalisations per day, unsustainable for any healthcare system. Large variations of S in a short time can reasonably occur only as a consequence of vaccination.

If we assume $\dot{S} \approx 0$, even in the short term we have that $\frac{d}{dt}\log(x(t)) \approx \bar{\lambda}\mathbf{1}$. Hence, "locally" we can write

$$\log(x(t + \delta t)) \approx \log(x(t)) + \mathbf{1}\bar{\lambda}\delta t \tag{16}$$

meaning that logarithmic curves tend to align and become parallel, over a short horizon.

The above predictions are well confirmed by the real data shown in Fig. 2, which illustrate the evolution of the COVID-19 pandemic in Italy from February to December 2020. Even though the epidemic parameters have substantially changed due to different NPIs adopted over time, quite interestingly, the curves associated with the infected categories remain essentially parallel throughout the whole period.

A simple additional explanation is provided by the following intuitive reasoning. NPIs modify c, but leave F essentially unchanged. As long as S varies slowly, it can be assumed approximately constant over a short horizon, so that $\dot{x} \simeq (F + b\bar{S}c^\top)x$. Then, $x(t)$ tends to align to the dominant Frobenius eigenvector $\bar{x}$, $x(t) \approx \bar{x}e^{\lambda t}$, whose logarithm has parallel lines as graphs as in (16).

A. Estimating $\bar{\lambda}$

The common Lyapunov exponent $\bar{\lambda}$ is the Perron-Frobenius eigenvalue of $F + b\bar{S}c^\top$, which is a continuous function of the parameters, decreasing with $\bar{S}$. Note that

$$\begin{aligned} 0 &= \det(\lambda I - F - b\bar{S}c^\top) \\ &= \det(\lambda I - F)\det(I - b\bar{S}c^\top(\bar{\lambda} I - F)^{-1}) \\ &= \det(\lambda I - F)(1 - \bar{S}G(\lambda)), \end{aligned}$$

where $G(\lambda) = c^\top(\bar{\lambda} I - F)^{-1}b$ is the transfer function from u to y evaluated in $\bar{\lambda}$. Therefore $\bar{\lambda} < 0$ is such that

$$G(\bar{\lambda})\bar{S} = 1, \tag{17}$$

with $G(0)\bar{S} = \mathcal{R}_0\bar{S} < 1$. The formula $G(\lambda)\bar{S} = 1$ yields any eigenvalue of $F + b\bar{S}c^\top$ that is not an eigenvalue of F. Being F Metzler and Hurwitz,

$$-\rho_s(F) < \bar{\lambda} < -\rho_s(F + b\bar{S}c^\top) < 0, \tag{18}$$

where ρ_s indicates the spectral abscissa.

B. Triangular epidemiological models

When F is a triangular compartmental matrix and $b = \mathbf{e}_1$, the exponent $\bar{\lambda}$ has a closed form expression in terms of $\bar{z}$, a right Frobenius eigenvector of $F + b\bar{S}c^\top$. Define a state-dependent reproduction function associated with the stationary point (i.e. $\dot{x}_1 = 0$) of the main infected stage x_1: at any time point, one can write

$$\lambda_1 = F_{11}(1 - \tilde{\mathcal{R}}_0 S), \quad \tilde{\mathcal{R}}_0 = -\frac{1}{F_{11}} c^\top \frac{x}{x_1}. \tag{19}$$

Then $\lambda_1 = 0$ when $\tilde{\mathcal{R}}_t = \tilde{\mathcal{R}}_0 S = 1$. Notice that $\tilde{\mathcal{R}}_0$ depends on the ratios x_i/x_j and is such that, when $\tilde{\mathcal{R}}_0 = 1/S$, the infected compartment x_1 has zero derivative. We have

$$\lim_{t\to\infty} \tilde{\mathcal{R}}_0 = -\frac{1}{F_{11}\bar{z}_1} c^\top \bar{z}, \quad \bar{\lambda} = F_{11} + c^\top \bar{S} \frac{\bar{z}}{\bar{z}_1},$$

to be compared with $\mathcal{R}_0 = -c^\top F^{-1} b$. If $n = 1$ (as for the SIR model) then

$$\mathcal{R}_0 = \tilde{\mathcal{R}}_0(x) = -\frac{c_1}{F_{11}}.$$

Example 1. *Consider a SIR-like model of the form* (1)-(4) *with*

$$F(\alpha, \beta, \gamma, \delta) = \begin{bmatrix} -\alpha & 0 & 0 \\ \alpha & -(\beta+\gamma) & 0 \\ 0 & \beta & -\delta \end{bmatrix},$$

$$b = \begin{bmatrix} 1 & 0 & 0 \end{bmatrix}^\top \text{ and } c^\top(\varphi, \mu, \nu) = \begin{bmatrix} \varphi & \mu & \nu \end{bmatrix}.$$

The contagion parameters are φ, μ, ν, while α, β, γ, δ are the flow parameters. Let $\alpha = 0.3$, $\beta = 0.1$, $\gamma = 0.1$, $\delta = 0.2$, $\varphi = 0.5$, $\mu = 0.2$, $\nu = 0.1$, so that the basic reproduction number is $\mathcal{R}_0 = 2.9167$. Take $x_1(0) = 0.01$, $S_0 = 0.99$, $x_2(0) = x_3(0) = 0$. Figure 3, top left, shows the time evolution of the state variables S and x, with $x \to 0$ and $S \to \bar{S} = 0.0648$. Figure 3, top right, shows the time evolution of variable x_1 and of the reproduction functions $\mathcal{R}_t$ and $\tilde{\mathcal{R}}_t$. As expected, the peak of x_1 is achieved when $\tilde{\mathcal{R}}_t = 1$. Figure 3 also shows the time evolution of the ratios x_i/x_j (bottom left) and of the logarithmic functions λ_i, achieving consensus with $\bar{\lambda} = -0.1422$ (bottom right).

Remark 2. *Assuming that the variation of susceptible people S is mainly due to vaccination leads to the system*

$$\dot{x}(t) = [Fx(t) + \bar{S}(t)bc^\top]x(t),$$

where $\bar{S}(t)$ is the residual portion of non-vaccinated people. For $\dot{S}$ small, all the previous considerations hold.

IV. The contagion function

We define a contagion function as follows.

Definition 1. *$Z(x) = z^\top x$ is a contagion function if, for all $x \gg 0$, it decreases if $S < 1/\mathcal{R}_0$ and it increases if $S > 1/\mathcal{R}_0$.*

We have the following characterisation.

Proposition 3. *$Z(x) = z^\top x$ is a contagion function if and only if z is aligned with $c^\top F^{-1}$: $z^\top = -\sigma c^\top F^{-1}$, for some $\sigma > 0$.*

Proof: Necessity: for $S = 1/\mathcal{R}_0$ we must have

$$\dot{Z}(x) = z^\top \dot{x} = \left[z^\top F + S z^\top b c^\top\right] x \equiv 0,$$

or, equivalently, $z^\top F^{-1} + S z^\top b c^\top = 0$. Since $S z^\top b$ is a scalar, $z^\top F$ must be aligned with $c^\top$.
Sufficiency: the derivative is

$$\begin{aligned} \dot{Z}(x) &= -\sigma c^\top F^{-1}\dot{x} = \sigma c^\top x + \sigma c^\top F^{-1} b c^\top x \\ &= \sigma\left[1 + c^\top F^{-1} b\right] c^\top x = \sigma\left[1 - S\mathcal{R}_0\right] c^\top x. \end{aligned}$$

Hence, decreasing or increasing Z corresponds to $S < 1/\mathcal{R}_0$ or $S > 1/\mathcal{R}_0$ respectively. ∎

Remark 3. *Since $Z(b) = \mathcal{R}_0$, we can say that $Z(x)$ increases (decreases) iff $Z(b) > 1$ ($Z(b) < 1$).*

Example 2. *The contagion function for Example 1 is defined by vector*

$$z^\top = \left[\frac{\phi}{\alpha} \quad \frac{\mu}{\beta+\gamma} \quad \frac{\beta\nu}{(\beta+\gamma)\delta}\right].$$

The contagion function can be leveraged to guide the implementation of open-close control strategies [10]. We can rewrite the susceptible equation as

$$\dot{S}(t) = -S(t)\kappa(t)c_0^\top x(t), \tag{20}$$

where $c(t) = \kappa(t)c_0$ and $\kappa(t) \in [\kappa^-, \kappa^+]$ can be modified by tightening or loosening the imposed restrictions. Although varying κ changes the value of c, we can consider the constant c_0 and the contagion function

$$Z(x) = -c_0^\top F^{-1} x.$$

Given upper and lower bounds $0 < \zeta^- < \zeta^+$ for $Z(x)$, we can apply the following hysteresis strategy:

$$\begin{aligned} &\text{if } Z(x(t)) > \zeta^+, \quad \text{switch to } \kappa = \kappa^- \quad \text{(close)} \\ &\text{if } Z(x(t)) < \zeta^-, \quad \text{switch to } \kappa = \kappa^+ \quad \text{(open)} \\ &\text{else } \kappa(t) = \kappa(t^-) \quad \text{(do not switch)}, \end{aligned}$$

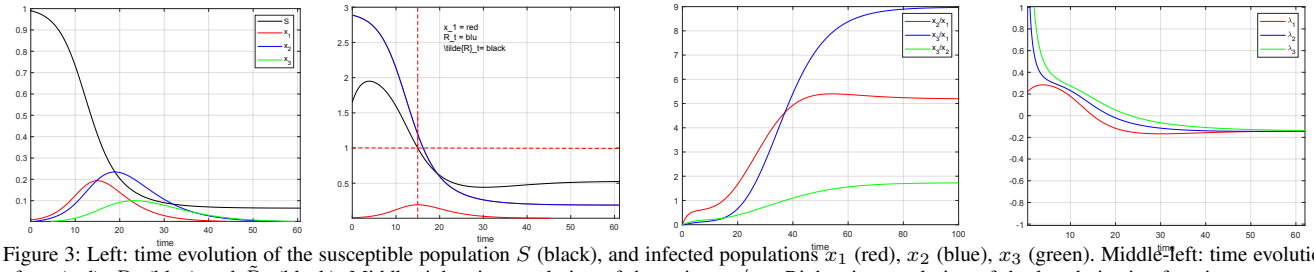

Figure 3: Left: time evolution of the susceptible population S (black), and infected populations x_1 (red), x_2 (blue), x_3 (green). Middle-left: time evolution of x_1 (red), R_t (blue) and $\tilde{R}_t$ (black). Middle-right: time evolution of the ratios x_i/x_j. Right: time evolution of the log-derivative functions.

which ensures that the region

$$\zeta^- \leq Z(x) \leq \zeta^+$$

is attractive and positively invariant.

V. Reduction to SI

By considering a state transformation, we can rewrite the general model (1)-(4) as only two scalar equations. Let

$$I := \frac{w^\top x}{w^\top b}$$

where $w \gg 0$ and $w^\top F \ll 0$. Taking the derivative yields

$$\dot{S} = -\alpha S I \quad (21)$$
$$\dot{I} = \alpha S I - \beta I \quad (22)$$
$$\beta = -\frac{w^\top F x}{w^\top x} \quad (23)$$
$$\alpha = w^\top b \frac{c^\top x}{w^\top x} \quad (24)$$

System (21)-(22) is not formally an SI model, since parameters α and β depend on $x = (I - \frac{bw^\top}{w^\top b})x + bI$. Still, one can define a reproduction number (function) $\mathcal{R}_w = \alpha/\beta$ associated with w such that $\dot{I} = 0$ (I has a peak) when $\mathcal{R}_w S = 1$.

Before providing interesting exemplifications for w, we provide upper and lower bounds for α and β.

Proposition 4. *Denoting by* $\min_i[v]$ *and* $\max_i[v]$ *the minimal and maximal components of* v*, it holds that*

$$\min_i \frac{[-w^\top F]_i}{[w^\top]_i} \leq \beta \leq \max_i \frac{[-w^\top F]_i}{[w^\top]_i} \quad (25)$$
$$w^\top b \min_i \frac{[c^\top]_i}{[w^\top]_i} \leq \alpha \leq w^\top b \max_i \frac{[c^\top]_i}{[w^\top]_i} \quad (26)$$

Proof: To prove the proposition, for the maximum case, it is sufficient to show that, given two vectors $p^\top \gg 0$ and $q^\top \gg 0$, it holds that $\mu^* \doteq \max \frac{p^\top x}{q^\top x} = \max_i \frac{p_i}{q_i}$. First, we note that μ^* is not smaller than $\max_i \frac{p_i}{q_i}$ because this value is achieved.

We prove that μ^* is not greater. Scaling x as ωx does not change the function: $p^\top x/q^\top x = p^\top(\omega x)/q^\top(\omega x)$. Then, we can constrain the optimisation problem in the cube

$$\mu^* = \sup_{0<x_i\leq 1} \frac{p^\top x}{q^\top x}.$$

For all x, $p^\top x \leq \mu^* q^\top x$ or $\phi(x,\mu^*) \doteq p^\top x - \mu^* q^\top x \leq 0$ in the unit cube. But this means that $\phi(x,\mu^*) \leq 0$ at all the vertices of the unit cube [14]. Then, in particular, $\mathbf{e_k}$ is a vertex and $\phi(\mathbf{e_k},\mu^*) \leq \mathbf{0}$. This means $p^\top \mathbf{e_k} - \mu^* \mathbf{q}^\top \mathbf{e_k} \leq \mathbf{0}$, hence $\frac{p^\top \mathbf{e_k}}{q^\top \mathbf{e_k}} = \frac{p_k}{q_k} \leq \mu^*$. So the maximum μ^* is not smaller than $\max_i \frac{p_i}{q_i}$.

An analogous proof holds for the minimum case. ■

We consider some peculiar cases.

1) Constant α: Assume that $\dot{S}$ is given by equation (20), $\dot{S} = -\kappa c_0^\top x S$. Then,

$$I = \frac{\bar{c}^\top x}{\bar{c}^\top b}, \quad \beta = -\frac{\bar{c}^\top F x}{\bar{c}^\top x}, \quad \alpha = \kappa \bar{c}_0^\top b,$$

so α is independent of x: $\alpha \in [\alpha_{min}, \alpha_{max}]$, with $\alpha_{max} = \kappa_{max} \bar{c}^\top b$, $\alpha_{min} = \kappa_{min} c^\top b$.

2) Constant β: Let μ be the left Frobenius eigenvector of $\bar{F} = F$, i.e., $w^\top \bar{F} = \mu w^\top$. Then,

$$I = \frac{w^\top x}{w^\top b}, \quad \beta = -\mu, \quad \alpha = w^\top b \frac{c^\top x}{w^\top x},$$

so β is independent of x.

3) Triangular case: Assume that F is triangular and $b = \mathbf{e}_1$. By taking $w = \mathbf{e}_1$, we have

$$I = x_1, \quad \beta = -F_{11}, \quad \alpha = \frac{c^\top x}{x_1},$$

so β is independent of x. Note that $\frac{\alpha}{\beta} = \tilde{\mathcal{R}}_0$, defined in (19).

4) Constant $\alpha/\beta = u\bar{\mathcal{R}}_0 = -u\bar{c}^\top \bar{F}^{-1} b$: In this case,

$$I = \frac{-\bar{c}^\top \bar{F}^{-1} x}{\bar{\mathcal{R}}_0}, \quad \beta = -\frac{\bar{c}^\top x}{\bar{c}^\top \bar{F}^{-1} x}, \quad \alpha = \beta \mathcal{R}_0 = u\beta\bar{\mathcal{R}}_0.$$

Since the choice of I is associated with the contagion function, the ratio α/β is independent of x. Interestingly, this case reflects *open-close* strategies for NPIs [10] where the basic reproduction number $\mathcal{R}_0$ can switch from a minimum value $\mathcal{R}_{min} = -u_{min}\bar{c}^\top F^{-1} b$ to a maximum value $\mathcal{R}_{max} = -u_{max}\bar{c}^\top F^{-1} b$. Letting $\lambda := \dot{I}/I = -\beta + \alpha S = -\beta(1 - \mathcal{R}_0 S)$, from the definition of $\bar{\lambda}$ (Theorem 1) we have

$$\lim_{t\to\infty} \beta = -\frac{\bar{\lambda}}{1 - \mathcal{R}_0 \bar{S}}, \quad \lim_{t\to\infty} \alpha = -\frac{\bar{\lambda}\mathcal{R}_0}{1 - \mathcal{R}_0 \bar{S}}. \quad (27)$$

for any constant $\mathcal{R}_0$.

Consider now the following potential function

$$V = I + S - \frac{1}{\mathcal{R}_0}\log(S) = -\frac{\dot{S}}{\alpha S} + S - \frac{1}{\mathcal{R}_0}\log(S) > 0 \quad (28)$$

that is constant along the system trajectories if $\mathcal{R}_0$ is constant. The trajectories in the plane (S, I) satisfy

$$I - I_0 = -S + S_0 + \frac{1}{\mathcal{R}_0} \log(S/S_0). \tag{29}$$

Interestingly, this is the same formula that is well known for the standard SI model [9, Section 9.2].

Example 3. *In the SIDARTHE model [12], the state variable x includes 5 compartments: infected, diagnosed, asymptomatic, recognised and threatened. The global infected compartment is chosen as in Section V, case 3. The initial condition is $x_0 = 0.01\mathbf{e}_1$, $S_0 = 0.99$. Figure 4 shows the evolution of S and I for various values of $\mathcal{R}_0$, ranging from 1.07 to 3.30. It can be verified that the final value of β matches the value in (27). Values $\mathcal{R}_0 < 1$ are not considered since the variation of S with respect to S_0 is negligible in such cases.*

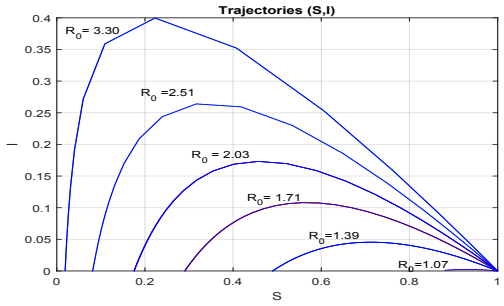

Figure 4: Trajectories in the (S, I) plane for various values of $\mathcal{R}_0$ for the SIDARTHE model [12].

VI. Conclusions

We have analysed class of generalised epidemiological systems, characterised by a linear compartmental model with a positive feedback due to the dynamics of the susceptible population. We have provided a theoretical justification for the empirically observed "parallel" behaviour of the compartmental infected variables represented in the logarithmic scale. Then, we have introduced some properly chosen functions of the state variables for aggregate analysis. These include the contagion function, whose decreasing/increasing behaviour is associated with $\mathcal{R}_t = \mathcal{R}_0 S$ being smaller/larger than 1, and the aggregate infected variable, which enables a planar analysis.

References

[1] T. Alamo, D. G. Reina, P. M. Gata, V. M. Preciado and G. Giordano, "Data-driven methods for present and future pandemics: Monitoring, modelling and managing", *Annual Rev. in Control*, 52, 448-464, 2021.

[2] J. Arino, F. Brauer, P. van den Driessche, J. Watmough and J. Wu, "A final size relation for epidemic models", *Mathematical Biosciences & Engineering*, 4(2), 159, 2007.

[3] F. Avram, R. Adenane and D. I. Ketcheson, "A review of matrix SIR Arino epidemic models", *Mathematics*, 9(13), 1513, 2021.

[4] M. Bin, P. Y. K. Cheung, E. Crisostomi, P. Ferraro, H. Lhachemi, R. Murray-Smith, C. Myant, T. Parisini, R. Shorten, S. Stein and L. Stone, "Post-lockdown abatement of COVID-19 by fast periodic switching", *PLoS Computational Biology*, 17(1), 2021.

[5] F. Blanchini, P. Bolzern, P. Colaneri, G. De Nicolao and G. Giordano, "Generalized epidemiological compartmental models: guaranteed bounds via optimal control", *IEEE Conf. on Dec. and Contr.*, 2021.

[6] F. Blanchini, P. Bolzern, P. Colaneri, G. De Nicolao and G. Giordano, "Optimal control of compartmental models: the exact solution", *Automatica*, accepted.

[7] F. Blanchini, P. Colaneri and M. E. Valcher, *Switched Linear Positive Systems*, Foundations and Trends in Systems and Control, 2(2), 101-273. 2016.

[8] M. Bloem, T. Alpcan and T. Basar, "Optimal and robust epidemic response for multiple networks", *Control Engineering Practice*, 17, 525-533, 2009.

[9] F. Brauer and C. Castillo-Chavez. *Mathematical Models in Population Biology and Epidemiology*. 2nd ed., Springer, 2012.

[10] G. De Nicolao, M. Colaneri, A. Di Filippo, F. Blanchini, P. Bolzern, P. Colaneri, G. Giordano and R. Bruno, "Preemptive periodic epidemic control reduces life and healthcare system costs without aggravation of social and economic losses", arXiv:2104.05597, April 2021.

[11] O. Diekmann and J. A. P. Heesterbeek. *Mathematical Epidemiology of Infectious Diseases: Model Building, Analysis and Interpretation*, Wiley, 2000.

[12] G. Giordano, F. Blanchini, R. Bruno, P. Colaneri, A. Di Filippo, A. Di Matteo and M. Colaneri, "Modelling the COVID-19 epidemic and implementation of population-wide interventions in Italy", *Nature Medicine*, 26, 855-860, 2020.

[13] G. Giordano, M. Colaneri, A. Di Filippo, F. Blanchini, P. Bolzern, G. De Nicolao, P. Sacchi, P. Colaneri and R. Bruno, "Modeling vaccination rollouts, SARS-CoV-2 variants and the requirement for non-pharmaceutical interventions in Italy", *Nature Medicine*, 27, 993-998, 2021.

[14] G. Giordano, C. Cuba Samaniego, E. Franco and F. Blanchini, "Computing the structural influence matrix for biological systems", *Journal of Mathematical Biology*, 72(7), 1927-1958, 2016.

[15] A. B. Gumel et al. ,"Modelling strategies for controlling SARS outbreaks", *Proc. R. Soc. B Biol. Sci.*, 271(1554), 2223-32, 2004.

[16] E. Hansen and T. Day, "Optimal control of epidemics with limited resources", *Journal of Mathematical Biology*, 62, 423-451, 2011.

[17] M. Hayhoe, F. Barreras and V. Preciado, "Data-driven control of the COVID-19 outbreak via non-pharmaceutical interventions: A geometric programming approach", arXiv 2011.01392, 2020.

[18] H. W. Hethcote, "The mathematics of infectious diseases", *SIAM Rev.*, 42, 599-653, 2000.

[19] W. O. Kermack and A. G. McKendrick, "A contribution to the mathematical theory of epidemics", *Proc. R. Soc. Lond.*, 115, 700-721, 1927.

[20] G. Leitmann, "The use of screening for the control of anendemic disease", in: Variational Calculus, Optimal Control and Applications. volume 124 of International Series of Numerical Mathematics, Birkhauser, pp. 291–300, 1998.

[21] S. Lenhart and J. T. Workman. *Optimal control applied to biological models*. Chapman and Hall, CRC, 2007.

[22] H. Maeda, S. Kodama and Y. Ohta, "Asymptotic behavior of nonlinear compartmental systems: Nonoscillation and stability", *IEEE Transactions on Circuits and Systems*, 25(6), 372–378, 1978.

[23] M. Mandal, S. Jana, S. K. Nandi, A. Khatua, S. Adak and T. Kar, "A model based study on the dynamics of COVID-19: Prediction and control", *Chaos, Solitons and Fractals*, 136, 109889, 2020.

[24] M. Martcheva. *An Introduction to Mathematical Epidemiology*. Springer Science and Business Media LLC, 2015.

[25] R. Morton and K. H. Wickwire, "On the optimal control of a deterministic epidemic", *Advances in Applied Probability*, 6, 622-635, 1974.

[26] O. Sharomi and T. Malik, "Optimal control in epidemiology", *Annals of Operations Research*, 251, 55-71, 2017.

[27] L. Stella, A. P. Martínez, D. Bauso and P. Colaneri, "The role of asymptomatic infections in the COVID-19 epidemic via complex networks and stability analysis",*SIAM J. Control and Optimization*, 2022.

[28] A. Swierniak, U. Ledzewicz and H. Schattler, "Optimal Control for a Class of. Compartmental Models in Cancer Chemotherapy", *Int. J. Appl. Math. Comput. Sci.*, 13(3), 357–368, 2003.